Published in final edited form as:

Eur J Immunol. 2016 October ; 46(10): 2352–2362. doi:10.1002/eji.201646354.

Temporal increase in thymocyte negative selection parallels enhanced thymic SIRPα+ DC function

Charles J. Kroger[1], **Bo Wang**[1], and **Roland Tisch**[1,2]

[1]Department of Microbiology & Immunology, University of North Carolina at Chapel Hill School of Medicine, Chapel Hill, NC 27599 USA

[2]Lineberger Comprehensive Cancer Center, University of North Carolina at Chapel Hill School of Medicine, Chapel Hill, NC 27599 USA

Abstract

Dysregulation of negative selection contributes to T cell-mediated autoimmunity, such as type 1 diabetes. The events regulating thymic negative selection, however, are ill-defined. Work by our group and others suggest that negative selection is inefficient early in ontogeny and increases with age. This study examines temporal changes in negative selection and the thymic DC compartment. Peptide-induced thymocyte deletion *in vivo* was reduced in newborn versus 4 wk-old NOD mice, despite a similar sensitivity of the respective thymocytes to apoptosis induction. The temporal increase in negative selection corresponded with an elevated capacity of thymic antigen presenting cells to stimulate T cells, along with altered subset composition and function of resident DC. The frequency of SIRPα$^+$ and plasmacytoid DC (pDC) was increased concomitant with a decrease in CD8α$^+$ DC in 4 wk-old NOD thymi. Importantly, 4 wk-old versus newborn thymic SIRPα$^+$ DC exhibited increased antigen processing and presentation via the MHC class II but not class I pathway, coupled with an enhanced T cell stimulatory capacity not seen in thymic pDC and CD8α$^+$ DC. These findings indicate that the efficiency of thymic DC-mediated negative selection is limited early after birth, and increases with age paralleling expansion of functionally superior thymic SIRPα$^+$ DC.

Keywords

Autoimmunity; Dendritic cells; Diabetes; Thymus; Central tolerance

Introduction

T cell central tolerance is achieved by negative selection events ongoing within the thymus. Single positive thymocytes (SP) in the thymic medulla undergo apoptosis or anergy upon relatively high avidity/affinity binding of self-peptide-MHC complexes presented by thymic

Corresponding Author: Roland Tisch, Department of Microbiology and Immunology, 6th Floor Marsico Hall, 125 Mason Farm Road, Campus Box 7290, University of North Carolina at Chapel Hill, Chapel Hill, NC 27599-7290. (919) 966-4766 (phone); (919) 962-8103 (fax); rmtisch@med.unc.edu.

Conflict of interest:
The authors declare there are no conflicts of interest in this study.

antigen presenting cells (APC) [1, 2]. On the other hand, aberrant thymic negative selection is believed to contribute to T cell-mediated autoimmune diseases such as type 1 diabetes (T1D) [3–6]. T1D is characterized by pathogenic $CD4^+$ and $CD8^+$ T cells which target multiple autoantigens and peptide epitopes derived from the insulin producing β cells in the pancreas. The events regulating the efficiency of thymic negative selection in general, and specifically in T1D are unclear (reviewed in [7]).

Medullary thymic epithelial cells (mTEC) and DC are major APC driving negative selection. mTEC are specialized APC characterized by expression of the Autoimmune regulator (AIRE) transcription factor, which controls expression of peripheral tissue specific antigens (TSA) presented to SP [8–10]. A key role for thymic DC in mediating negative selection is demonstrated in mice that develop T cell-mediated autoimmunity upon DC ablation [11, 12]. Thymic DC primarily consist of $CD11c^+$ signal regulatory protein α^+ ($SIRP\alpha^+$) and $CD8\alpha^+$ conventional DC (cDC) subsets as well as plasmacytoid DC (pDC) (reviewed in [13]). Localized to the cortico-medullary junction, DC present TSA obtained by engulfment of apoptotic mTEC, intercellular transfer of peptide-MHC complexes from the surface of mTEC, and by uptake and processing of soluble antigens (Ag) in blood [14–18]. Negative selection is also mediated by self-Ag laden peripheral $SIRP\alpha^+$ DC and pDC that migrate into the thymus [19–22]. Although it is widely accepted that both mTEC and thymic DC are critical, the relative contribution of these APC in driving negative selection remains poorly defined [23, 24].

Recently we showed using a thymus transplant model that development of autoreactive T cells in NOD mice, a model of spontaneous T1D, is restricted to a narrow window early in ontogeny [25]. Diabetes developed in NOD.*scid* recipients of thymi transplanted from newborn but not 4 wk-old NOD mice, indicating that the efficiency of thymic negative selection increases with age. Early ontogenic development of β cell-specific T cells is further supported by observations that NOD mice continue to develop diabetes despite thymectomy at 3 d of age [26]. Furthermore, observations made in other models of T cell-mediated autoimmunity [27], and reports of autoimmunity in congenital athymic children receiving infant thymi transplants [28], also suggest that the efficiency of thymic negative selection is limited early in life. How thymic negative selection is regulated in a temporal manner, however, is unknown. In the current study, we demonstrate that temporal changes in the composition and function of thymic DC subsets, specifically within the $SIRP\alpha^+$ DC pool, parallel the increase in negative selection efficiency.

Results

In vivo induced thymic negative selection is enhanced with age in NOD mice

Inefficient thymic negative selection early after birth in NOD mice may explain the development of diabetes in NOD.*scid* mice transplanted with newborn but not 4 wk-old NOD thymi [25]. To test this hypothesis, sBDC mimetic peptide was administered i.v. into newborn and 4 wk-old NOD.BDC mice, which express the IA^{g7}-restricted BDC2.5 clonotypic TCR. Thymi were harvested 18 h post-injection and the frequency of apoptotic SP $CD4^+$ thymocytes (CD4SP) assessed by VAD-FMK. A peptide dose-dependent increase in VAD-FMK^+ CD4SP was seen in the thymus of 4 wk-old versus newborn NOD.BDC mice

(Fig. 1A,B). Consistent with this finding, sBDC-induced TCR signaling, based on the frequency of Nur77$^+$ CD4SP, was also significantly increased, up to 6-fold, in 4 wk-old NOD.BDC mice (Fig. 1C,D). Similarly, injection of hemagglutinin (HA) peptide increased VAD-FMK$^+$ CD8SP in the thymi of 4 wk-old versus newborn NOD.CL4 mice, which express an H2K^d-restricted, HA-specific TCR (Fig. 1E).

Previous studies have examined the sensitivity of double positive thymocytes (DP) to antigen-stimulated apoptosis as an additional indicator of clonal deletion efficiency [18, 29]. Accordingly, the frequency of sBDC-induced apoptosis of DP in NOD.BDC mice was measured. Similar to CD4SP, a significant increase in the percent of VAD-FMK$^+$ DP was detected in 4 wk-old versus newborn thymi (Fig. 1F). Next, to determine if the temporal difference in peptide-induced apoptosis of thymocytes was a general observation and independent of the NOD genotype, C57BL/6 mice congenic for H2^{g7} and expressing the BDC2.5 TCR transgene (B6^{g7}.BDC) were examined. Similar to NOD mice, up to a 4-fold increase in VAD-FMK$^+$ DP was seen in thymi of 4 wk-old versus newborn B6^{g7}.BDC mice injected with sBDC (Fig. 1G).

The limited increase in apoptotic thymocytes in newborn animals was not due to enhanced clearance of apoptotic cells. For example, a similar frequency of VAD-FMK$^+$ SP was detected in newborn and 4 wk-old NOD animals treated with dexamethasone, which induces thymocyte apoptosis (Fig. 1H). Alternatively, the above age-dependent increase in thymic deletion may be due to elevated sensitivity of thymocytes to peptide-induced apoptosis. Accordingly, NOD.BDC thymocytes from newborn and 4 wk-old mice were co-cultured with sBDC-pulsed thymic DC from 4 wk-old NOD mice, and the frequency of VAD-FMK$^+$ cells determined. Interestingly, induction of apoptosis was increased in newborn versus 4 wk-old CD4SP at low (but not higher) sBDC concentrations (Fig. 1I). Collectively, these results demonstrate that peptide-induced CD4SP and CD8SP (and DP) apoptosis is enhanced in 4 wk-old versus newborn thymi, and independent of: i) genotype, ii) SP sensitivity to antigenic stimulation, and iii) apoptotic thymocyte clearance.

A temporal increase in thymic APC stimulatory capacity is due to resident DC

One scenario to explain the enhanced peptide-induced SP apoptosis in 4 wk-old animals is a concomitant increase in the stimulatory capacity of thymic APC. Whole thymic suspensions prepared from newborn and 4 wk-old NOD mice were pulsed with sBDC peptide, and co-cultured with CFSE-labeled splenic NOD.BDC CD4$^+$ T cells. *In vitro* treatment of the thymic suspensions ensured uniform peptide-pulsing of APC. Proliferation of CD4$^+$ T cells was increased at limiting sBDC concentrations with 4 wk-old versus newborn thymic suspensions (Fig. 2A). Examination of the thymus cellular composition showed an increased frequency of thymic DC (CD11c$^{int/hi}$), and an elevated ratio of thymic DC to thymocytes in 4 wk-old versus newborn thymic suspensions (Fig. 2B,C). These results suggested that thymic DC contribute to the temporal increase in T cell stimulation and in turn negative selection efficiency. Accordingly, CD11c$^+$ DC were depleted with magnetic beads (Fig. 2B), and the T cell stimulatory capacity of 4 wk-old thymus suspensions compared to unmanipulated thymus suspensions. DC depletion reduced CD4$^+$ T cell proliferation in 4 wk-old thymus suspensions, which was comparable to unmanipulated newborn thymic

suspensions (Fig. 2A). On the other hand, depleting DC from newborn thymic suspensions only minimally reduced T cell proliferation (Fig. 2A).

To directly test the stimulatory capacity of thymic DC, newborn and 4 wk-old NOD mice were injected with titrated doses of sBDC, and isolated thymic DC co-cultured with CFSE-labeled NOD.BDC $CD4^+$ T cells. $CD4^+$ T cell proliferation was increased by thymic DC from 4 wk-old versus newborn mice injected with low sBDC doses (Fig. 2D). A similar trend of increased BDC $CD4^+$ T cell proliferation with thymic DC isolated from 4 wk-old versus newborn $B6^{g7}$ congenic mice injected with sBDC was also observed (Fig. 2E). Together these findings demonstrate that the T cell stimulatory capacity of thymic APC increases with age, which correlates with enhanced thymic DC function and frequency, and is independent of non-MHC genotype.

Thymic DC subsets exhibit distinct stimulatory capacities with age

The temporal increase in T cell stimulation by DC may be due to changes in phenotype and/or subset composition. Within the newborn and 4 wk-old thymic DC pools, however, no uniform age-dependent increase in surface expression of MHC class I and II, and co-stimulatory molecules (CD40, CD80, CD86) was observed; in fact expression of these molecules tended to be increased in newborn thymic DC (Fig. 3A,B). Similar results were obtained for the individual DC subsets (Supporting Information Fig. 1).

Temporal changes in the composition of the 3 thymic DC subsets, namely pDC ($CD11c^{int}PDCA^+/B220^+$), and conventional ($CD11c^{hi}$) $SIRP\alpha^+$ and $CD8\alpha^+$ DC were assessed. Initially, gating on the $CD11c^{int/hi}$ cells demonstrated distinct thymic DC composition in the different aged thymus (Fig. 3C); importantly, $B220^-SIRP\alpha^-$ DC expressed high levels of surface CD8α (Supporting Information Fig. 2). The NOD newborn thymus contained mostly $CD8\alpha^+$ DC (72.1±0.8%), whereas the remainder of the pool consisted of $SIRP\alpha^+$ DC (11.6±1.2%) and pDC (11.5±1.2%) (Fig. 3C). In 4 wk-old NOD thymi, however, a ≥2-fold increase in $SIRP\alpha^+$ DC (23.3±1.6%) and pDC (26.0±2.1%), and a concomitant decrease in $CD8\alpha^+$ DC (45.7±1.0%) was seen (Fig. 3C).

To test the stimulatory capacity of the respective thymic DC subsets, $CD8\alpha^+$ DC, $SIRP\alpha^+$ DC and pDC were sorted by flow cytometry from newborn and 4 wk-old NOD mice 18 h post-injection of sBDC, and NOD.BDC $CD4^+$ T cell proliferation measured *in vitro*. Thymic pDC stimulated the lowest T cell proliferation, and no difference was observed between newborn and 4 wk-old pDC (Fig. 3D). Thymic $CD8\alpha^+$ DC displayed an increased capacity to induce $CD4^+$ T cell proliferation relative to pDC, but again no marked difference in stimulatory capacity was detected between newborn and 4 wk-old $CD8\alpha^+$ DC (Fig. 3D). On the other hand, 4 wk-old versus newborn $SIRP\alpha^+$ DC elicited a significant increase in $CD4^+$ T cell proliferation (Fig. 3D). Furthermore, T cell proliferation was increased ~2-fold by $SIRP\alpha^+$ versus $CD8\alpha^+$ DC from 4 wk-old thymi (Fig. 3D). These findings indicate that the temporal increase in frequency and stimulatory function of $SIRP\alpha^+$ DC contribute to the enhanced negative selection seen in peptide-treated 4 wk-old animals (Fig. 1).

In vivo and *in vitro* Ag processing by thymic SIRPα$^+$ DC increases with age

Thymic DC, particularly SIRPα$^+$ DC, acquire, process and present blood borne self-Ag to thymocytes [16–18, 30]. With this in mind, we determined if a temporal difference existed in thymic DC Ag uptake, processing and presentation/stimulation. Initially, the frequency of fluorescent thymic DC after injection of ovalbumin Alexa Fluor 647 (OVA-647) normalized for body weight (e.g. 2.7 mg/kg) was assessed for newborn and 4 wk-old NOD mice. Here, the loss of fluorescence over time was used as a measure of OVA-647 processing [31]. A small fraction, ~5% and 10% of thymic pDC and CD8α$^+$ DC, respectively, were OVA-647$^+$ at 1 h post-injection, after which the frequency decreased indicating proteolytic OVA-647 processing (Fig. 4A,B). The temporal loss of OVA-647$^+$ pDC and CD8α$^+$ DC was similar in newborn and 4 wk-old NOD mice (Fig. 4A,B). Strikingly, a 4–6-fold increase in the frequency of OVA-647$^+$ for both newborn and 4 wk-old SIRPα$^+$ DC was detected 1 h post-injection compared to pDC and CD8α$^+$ DC (Fig. 4A–C). Furthermore, OVA-647 was rapidly degraded in 4 wk-old SIRPα$^+$ DC resulting in an ~3-fold decrease in the frequency of fluorescent cells over time (Fig. 4C). In contrast, OVA-647$^+$ cells were reduced by only ~10% for newborn SIRPα$^+$ DC over time (Fig. 4C), indicating that *in vivo* exogenous Ag processing varies with age for thymic SIRPα$^+$ DC.

To directly determine if differences in protein processing following Ag uptake existed, newborn and 4 wk-old thymic DC were co-cultured with DQ-ovalbumin (DQ-OVA) *in vitro*. Unlike OVA-647, DQ-OVA is initially non-fluorescent but upon proteolytic degradation emits a fluorescent signal, used to measure the efficiency of protein processing [32]. Consistent with the *in vivo* data, the frequency of DQ-OVA$^+$ fluorescent SIRPα$^+$ DC from 4 wk-old versus newborn NOD mice was increased (Fig. 4F). No difference, however, was detected in the frequency of fluorescent thymic pDC or CD8α$^+$ DC between newborn and 4 wk-old NOD thymi, which in turn was reduced relative to SIRPα$^+$ DC (Fig. 4D–F). Furthermore, no age-dependent differences were observed for a given DC subset regarding: i) mannose receptor (CD206) expression which binds to and internalizes OVA [33, 34] and ii) OVA-647 binding and uptake at 4° or 37° C after a 30 min incubation *in vitro* (data not shown). These results indicate that a temporal difference in Ag processing exists between newborn versus 4 wk-old thymic DC, which is mediated by SIRPα$^+$ DC.

Stimulatory function of thymic SIRPα$^+$ DC increases with age for Ag processed via the MHC class II but not class I pathway

Whether the enhanced Ag processing by 4 wk-old thymic DC correlates with increased T cell stimulation was next investigated. Newborn and 4 wk-old total thymic DC were pulsed with hen egg lysozyme (HEL) protein, co-cultured with Clone 4 T cells, an IA^{g7}-restricted CD4$^+$ T cell hybridoma specific for HEL$_{11–25}$ [30], and IL-2 secretion measured. Consistent with the above OVA processing data (Fig. 4), thymic DC from 4 wk-old NOD mice induced significantly higher IL-2 secretion compared to newborn thymic DC (Fig. 5A). Furthermore, T cell stimulation was dependent on Ag processing; treatment of 4 wk-old thymic DC with a cocktail of protease inhibitors blocked HEL protein-induced IL-2 secretion by Clone 4 T cells (Fig. 5B). To determine if age-dependent changes in Ag processing and T cell stimulation could also be detected *ex vivo,* newborn and 4 wk-old NOD mice were injected with HEL protein and thymic DC isolated. Similar to pulsing DC with HEL protein *in vitro*

(Fig. 5A), 4 wk-old versus newborn thymic DC from HEL protein injected animals stimulated up to a 4-fold increase in IL-2 secretion by Clone 4 T cells (Fig. 5C,D).

Notably, the temporal increase in OVA and HEL processing by 4 wk-old thymic DC correlated with changes in mRNA expression of proteases associated with the MHC class II protein processing and presentation pathway (Fig. 5E). 4 wk-old versus newborn thymic DC had a 5-fold reduction in mRNA levels of the thymus specific serine protease (TSSP), and ~3-fold increase in cathespin S (CatS) levels (Fig. 5E). H2DMα/β expression, however, was comparable in 4 wk-old versus newborn thymic DC (Fig. 5E). Expression of molecules associated with the MHC class I Ag processing and presentation pathway, including components of the immunoproteosome, was similar for newborn and 4 wk-old thymic DC (Fig. 5E). Thus, the temporal increase in $CD4^+$ T cell stimulatory capacity of 4 wk-old thymic DC correlated with changes in mRNA expression of proteases associated with the MHC class II Ag processing and presentation pathway.

The above results for OVA processing (Fig. 4) suggested a scenario in which the increase in HEL-specific T cell stimulation by 4 wk-old thymic DC (Fig. 5A,C,D) was due to $SIRP\alpha^+$ DC. To test this, newborn and 4 wk-old thymic pDC, $CD8\alpha^+$ and $SIRP\alpha^+$ DC were sorted by flow cytometry and pulsed with 125 μg/ml HEL protein *in vitro*, and T cell stimulatory function measured. Thymic pDC induced only minimal Clone 4 T cell IL-2 secretion, although an increased albeit variable stimulatory capacity was seen for 4 wk-old versus newborn pDC (Fig. 5F,G). Thymic $CD8\alpha^+$ DC exhibited an increased stimulatory function relative to thymic pDC that was, however, similar between newborn and 4 wk-old $CD8\alpha^+$ DC (Fig. 5F,G). Notably, 4 wk-old versus newborn $SIRP\alpha^+$ DC induced ~3–4 fold greater IL-2 secretion by Clone 4 T cells (Fig. 5F,G).

We then determined if Ag cross-presentation by thymic DC also varied with age. Sorted DC subsets were co-cultured with HEL protein and the $CD8^+$ T cell hybridoma Clone 8c11, specific for the $H2D^b$-restricted $HEL_{23–31}$ epitope. Regardless of age, pDC stimulated only minimal IL-2 secretion (Fig. 5H). Compared to pDC, $SIRP\alpha^+$ DC induced higher IL-2 secretion but no difference between newborn and 4 wk-old $SIRP\alpha^+$ DC was detected (Fig. 5H). Thymic $CD8\alpha^+$ DC were the most efficient at cross-presenting HEL protein, resulting in >5-fold increase of IL-2 secretion by Clone 8c11 T cells compared to age-matched pDC and $SIRP\alpha^+$ DC (Fig. 5H). However, no increase in IL-2 was stimulated by 4 wk-old thymic $CD8\alpha^+$ DC; in fact newborn $CD8\alpha^+$ DC trended towards an enhanced stimulatory capacity (Fig. 5H). Together these results demonstrate that increased Ag processing by 4 wk-old thymic DC, and specifically $SIRP\alpha^+$ DC, is concomitant with an increased stimulatory capacity of $CD4^+$ T cells *in vitro* and *ex vivo*, not seen for cross-presented Ag.

Discussion

The goal of this work was to gain insight into the temporal events influencing the efficiency of thymocyte negative selection. Studies by our group and others [25, 26] indicate that the majority of autoreactive T cell development in NOD mice is restricted to a window early in ontogeny, and that the efficiency of negative selection increases with age. The current study provides further support for this model. Peptide-induced apoptosis of SP and DP was

reduced in newborn mice relative to 4 wk-old animals (Fig. 1). Age-dependent differences in the efficiency of negative selection were also detected in $B6^{g7}$.BDC mice (Fig. 1) demonstrating that these changes are not unique to the NOD genotype. Indeed inefficient negative selection early in ontogeny has been reported in B6 mice expressing a transgenic myelin basic protein-specific TCR [27].

How then is thymic negative selection regulated in an age-dependent manner? Our results rule out a temporal increase in the sensitivity of SP to apoptosis induced in an antigen-independent (Fig. 1H) and dependent (Fig. 1I) manner, as well as differences in thymic clearance of apoptotic thymocytes (Fig. 1H). Indeed, SP from 4 wk-old NOD mice had no increase in surface expression of pro-apoptotic molecules such as PD-1/PD-L1 and Fas/FasL (data not shown). Our findings implicate temporal changes within the thymic DC pool. Four wk-old versus newborn NOD thymus suspensions induced greater T cell proliferation (Fig. 2A) which: i) correlated with an increased frequency of thymic DC (Fig. 2B,C), and ii) was reduced by DC depletion (Fig. 2A). Furthermore, thymic DC isolated from 4 wk-old NOD mice injected with peptide (Fig. 2D) or intact Ag (Fig. 5C,D) stimulated increased T cell proliferation or IL-2 production compared to newborn thymic DC. A previous study showed that Ag injected i.v. is captured and presented *in vivo* by thymic DC, and not mTEC [16]. Therefore under our experimental conditions, mTEC are expected to have a limited role. Our results, however, do not exclude the possibility that changes within mTEC or other thymic APC, such B cells and macrophages, also impact the efficiency of thymic negative selection in a temporal manner.

Marked temporal differences in the frequency and function were detected among the thymic DC subsets. The newborn thymus consisted mostly of $CD8\alpha^+$ DC (~70%), whereas the frequency of both $SIRP\alpha^+$ DC and pDC increased with age (Fig. 3C). This profile likely reflects the thymic origin of $CD8\alpha^+$ DC and the recruitment of migratory $SIRP\alpha^+$ DC and pDC from the periphery. An earlier study also reported a temporal increase in thymic pDC [35]. Under the conditions tested a hierarchy in T cell stimulatory capacity was seen among the thymic DC subsets from Ag-injected animals, which was age-dependent. Sorted thymic pDC from peptide-injected mice or pulsed with intact Ag *in vitro* were the least stimulatory (Figs. 3D, 5) and expressed the lowest levels of MHC and co-stimulatory molecules (e.g. CD40, CD80, CD86) among the 3 thymic DC subsets (Supporting Information Fig. 1). Thymic $CD8\alpha^+$ DC stimulated T cells to a greater extent but neither $CD8\alpha^+$ DC nor pDC showed increased stimulatory activity with age. Newborn thymic $SIRP\alpha^+$ DC exhibited comparable stimulatory activity to either newborn or 4 wk-old $CD8\alpha^+$ DC (Figs. 3D, 5). However, the stimulatory capacity of 4 wk-old thymic $SIRP\alpha^+$ DC was increased relative to newborn $SIRP\alpha^+$ DC and 4 wk-old $CD8\alpha^+$ DC (and pDC) (Figs. 3D, 5F,G). Our findings support a scenario in which the temporal increase in the frequency and stimulatory activity of $SIRP\alpha^+$ DC contribute to enhanced negative selection. Reduced peptide-induced apoptosis of thymocytes has been reported in CCR2 knockout mice, which have a decreased frequency of thymic $SIRP\alpha^+$ DC, further supporting a key role for this thymic DC subset in negative selection [18].

Intrinsic and extrinsic factors likely contribute to the enhanced stimulatory function of $SIRP\alpha^+$ DC over time. The latter, however, was independent of any marked increase in

surface expression of MHC class I and II, as well as the co-stimulatory molecules CD40, CD80, and CD86 on 4 wk-old versus newborn thymic SIRPα$^+$ or CD8α$^+$ DC (Supporting Information Fig. 1). However, the possibility that expression of other costimulatory molecules may vary temporally and contribute to changes in the stimulatory capacity of SIRPα$^+$ DC cannot be ruled out. Notably, SIRPα$^+$ DC in adult mice are localized next to blood vessels at the cortico-medullary junction and within the medulla, which is expected to enhance capture of blood borne Ag [18] such as OVA-647 and HEL. Indeed, a 4–6-fold increase in the frequency of fluorescent SIRPα$^+$ DC was detected in newborn and 4 wk-old NOD mice relative to CD8α$^+$ DC and pDC shortly after OVA-647 injection (Fig. 4A–C). Differences in circulating Ag uptake or presentation among thymic SIRPα$^+$ DC, CD8α$^+$ DC and pDC have also been reported [16–18].

Strikingly, an age-dependent increase in Ag processing was also seen for thymic SIRPα$^+$ DC but not other DC subsets. Processing of OVA-647 and DQ-OVA *in vivo* and *in vitro* was increased in 4 wk-old versus newborn SIRPα$^+$ DC (Fig. 4C,F), whereas age-dependent differences among thymic CD8α$^+$ DC and pDC were only minimal. This increased Ag processing activity correlated with enhanced CD4$^+$ T cell stimulation (Fig. 5F,G). Interestingly, temporal differences in mRNA expression were detected in thymic DC for molecules associated with MHC class II but not class I Ag processing and presentation (Fig. 5E). Decreased TSSP expression, coupled with an increase in expression of CatS would be expected to elevate the stimulatory capacity of 4 wk-old thymic DC, and the efficiency of negative selection (Fig. 5E). For example, TSSP expressed by thymic DC has been shown to limit presentation of certain β cell-derived peptides, and TSSP deficiency enhances negative selection in transgenic NOD thymocytes depending on the epitopes recognized by β cell-specific TCR [37]. Furthermore, β cell autoimmunity is blocked in NOD mice lacking TSSP expression [6, 37, 38]. Elevated expression of CatS, which drives the proteolytic degradation of the invariant chain [39–43] would be predicted to increase the number of “empty” MHC class II complexes, and improve the loading of self-peptides by 4 wk-old thymic DC. Altered expression of various components of the MHC II Ag processing machinery is expected to have both quantitative and qualitative effects on the presentation of autoantigenic peptide-MHC complexes that influence the efficiency of negative selection of self-specific CD4SP clonotypes. Additional experiments are needed to better define how temporal differences in TSSP and CatS influence thymic DC Ag presentation.

Multiple parameters, including an altered thymic SIRPα$^+$ DC pool, are expected to contribute to the age-dependent increase in negative selection. For instance, the structural organization of the thymus undergoes marked changes with age that likely impact the efficacy of negative selection [25]. By 4 wk of age, the murine thymus contains large, well-formed medulla regions. In contrast, the newborn thymic architecture consists of small poorly defined medulla with small clusters of mTEC and DC, which may limit dwell times and the avidity of interactions between thymic APC and SP. Ontogenic changes in mTEC, such as increases in the frequency of mature mTEC and/or expression of TSA may also promote increased negative selection. For example, AIRE expression by mTEC is critical early but not later in ontogeny to prevent autoimmunity [44]. Concomitant changes in APC function for thymic DC and mTEC may reflect a “division of labor” [45]. Here mTEC drive negative selection via expression and presentation of TSA whereas thymic DC, particularly

SIRPα$^+$ DC, promote negative selection to self-Ag captured from blood or ferried from the periphery. Similarly, the respective thymic DC subsets may have specialized roles in mediating negative selection and/or promoting Foxp3$^+$Treg development, which in turn depend on how self-Ag is acquired [16, 17]. An increased capacity to capture soluble Ag (e.g. SIRPα$^+$ DC), acquire peptide-MHC complexes from the surface of mTEC, and/or uptake of apoptotic mTEC may favor a given thymic DC subset. Indeed, thymic CD8α$^+$ DC demonstrated increased cross-presentation of exogenous Ag to CD8$^+$ T cells relative to SIRPα$^+$ DC and pDC (Fig. 5H) similar to peripheral CD8α$^+$ DC [46]. Interestingly, the efficiency of cross-presentation was not significantly affected by age, consistent with the lack of age-dependent changes in gene expression of MHC class I processing molecules (Fig. 5E). The latter further highlights the selectivity of the ontogenic changes within thymic SIRPα$^+$ DC. Additional studies are needed to define the basis for the temporal increase in Ag processing and presentation by SIRPα$^+$ DC. It is possible that expression of local or "licensing" factors [47] that promote enhanced Ag processing by thymic SIRPα$^+$ DC are increased in an age-dependent manner.

These results provide novel insight into the temporal regulation of negative selection. Our findings demonstrate that the age-dependent increase in the efficiency of negative selection is in part attributed to quantitative and qualitative changes within the thymic SIRPα$^+$ DC pool. We propose a model in which efficacy of negative selection in the thymus early after birth is enhanced by an increase in thymic SIRPα$^+$ DC which traffic from the periphery and localize to blood vessels within the cortico-medullary junction and medulla. This positioning facilitates efficient sampling of blood borne self-Ag, which coupled with a temporal increase in Ag processing and presentation, leads to enhanced negative selection of SP. These observations underscore the complex and dynamic nature of T cell central tolerance.

Materials and Methods

Mice and cell lines

NOD/LtJ (NOD), C57BL/6.*H2*^{g7} (B6^{g7}), NOD.Cg-Tg(TcraBDC2.5)1Doi Tg(TcrbBDC2.5)2Doi/DoiJ (NOD.BDC), and NOD.Cg-*Thy1*^{a}/*Thy1*^{b} Tg(TcraCl4, TcrbCl4)1Shrm/ShrmJ (NOD.CL4) mice were bred and maintained in specific pathogen-free facilities at the University of North Carolina at Chapel Hill (UNC-CH). B6^{g7} and B6^{g7}.BDC mice were a kind gift from Drs. Mathis and Benoist. Mouse experiments were approved by the UNC-CH Institutional Animal Care and Use Committee. Clone 4 and Clone 8c11 T cell hybridomas were a kind gift from Dr. Unanue [30].

Flow cytometry

All Ab were purchased from eBioscience, BD Biosciences, or Biolegend. Staining was measured with a Beckman-Coulter Cyan (Dako) or BD LSR II, and results analyzed with Summit (Dako) or FlowJo software. Cells were stained with Pacific Orange succinimidyl ester (Invitrogen), LIVE/DEAD fixable blue dead cell stain (Invitrogen) or 7AAD (BD Biosciences) to exclude dead cells. For analyses of DC subsets, live cells were gated on and autofluorescent cells excluded in a dump channel. pDC were identified as CD11c^{int} (N418), B220$^+$ (RA3-6B2)/PDCA$^+$ (927) or CD45RA$^+$ (14.8). cDC were identified as CD11c^{hi} and

separated based on SIRPα (P84) and CD8α (53-6.7) expression. SIRPα$^+$ DC were identified as CD11c^{hi} SIRPα$^+$, whereas CD8α$^+$ DC were classified as CD11c^{hi}SIRPα$^-$/CD8α$^+$.

Thymocyte negative selection assays

Newborn and 4 wk-old NOD.BDC or NOD.CL4 mice were injected i.v. with peptide via the percutaneous vein [48] or lateral tail vein, and 18 h later single cell thymus suspensions prepared. To measure apoptosis, thymocytes were stained with CaspACE FITC-VAD-FMK (Promega) or anti-Nur77 (12.14), and CD4 (RMA4-4), –CD8α and –CD69 (H1.2F3) Ab. Anti-Vβ4 (KT4) and -Vβ8.1/8.2 (MR5-2) Ab were used to identify clonotypic BDC and CL4 thymocytes, respectively. Thymocytes were fixed/permeabilized for intracellular Nur77staining. For *in vitro* negative selection assays, bulk thymic DC (2×10^4) isolated from 4 wk-old donors (see below) were pulsed with sBDC for 1 h, washed, co-cultured with NOD.BDC newborn or 4 wk-old thymocytes (2×10^5) for 6 h at 37°C, and thymocyte apoptosis measured via flow cytometry.

Thymic DC isolation and analyses

Newborn and 4 wk-old thymi were digested with collagenase D (0.5 mg/mL) and DNase I (5 μg/mL; Roche) for 30 min at 37°C, and total thymic DC isolated using anti-CD11c magnetic beads (Miltenyi Biotech) as per the manufacturer's directions; DC purity was typically ~90%. Alternatively, thymic DC subsets defined as above were sorted by flow cytometry using a Beckman-Coulter MoFlo (Dako) or FACsAria III (BD Bioscience). DC maturation was assessed with Ab specific for CD40 (3/23), CD80 (16–10A1), CD86 (GL1), H2K^d (SF1–1.1), H2D^b (KH95), and IA^{g7} (10-3.6). In some experiments, thymic DC were isolated 18 h post i.v. injection of 10–250 μg sBDC peptide/mouse. To assess T cell stimulatory capacity, isolated DC were co-cultured at a 1:10 ratio with splenic BDC CD4$^+$ T cells purified with a CD4$^+$ T cell isolation kit (Miltenyi Biotech), and labeled with CFSE (Invitrogen). After 72 h, cells were stained with Pacific Orange live/dead cell marker, anti-CD4, -CD3 and -Vβ4, and proliferation measured by flow cytometry. Thymus suspensions, either unmanipulated or depleted of DC using anti-CD11c magnetic beads, were pulsed with sBDC, and co-cultured with CFSE-labeled splenic BDC CD4$^+$ T cells at a 1:10 ratio for 72 h.

Analyses of thymic DC Ag processing

OVA processing—Newborn and 4 wk-old NOD mice were injected i.v. with 2.7 mg/kg body weight (3.5 and 50 μg, respectively) of OVA-647 (Invitrogen), and OVA-647$^+$ thymic DC analyzed by flow cytometry. In addition, purified thymic DC ($2.5–5\times10^4$) were cultured with 0.5 μg/well of DQ-OVA (Invitrogen), and analyzed by flow cytometry.

HEL processing—Newborn and 4 wk-old NOD mice were injected with 2.7 or 27 mg/kg body weight of HEL protein (Sigma), respectively, and thymic DC isolated 30 min later by anti-CD11c magnetic beads. Alternatively, total thymic DC or sorted thymic DC subsets were: i) incubated with HEL protein for 30 min at 37°C, washed and co-cultured at a 1:1 ratio with Clone 4 CD4$^+$ T cells in the presence or absence of a protease inhibitor cocktail (Sigma), or ii) co-cultured with HEL protein and at a 1:1 ratio with Clone 8c11 CD8$^+$ T cells

for up 48 h. IL-2 secretion by Clone 4 or 8c11 T cells was then measured by ELISA as described [49].

Real-time PCR

NOD newborn and 4 wk-old thymic DC were enriched using anti-CD11c beads and RNA isolated with a Qiagen RNAeasy kit followed by cDNA synthesis. 100–200 ng of cDNA was utilized in real-time PCR reactions. Primer sequences are provided in Supporting Information Table 1. The fold increase in RNA expression levels of 4 wk-old over newborn thymic DC was calculated using the $2^{(-\Delta\Delta Ct)}$ method with β actin as the housekeeping reference gene.

Supplementary Material

Refer to Web version on PubMed Central for supplementary material.

Acknowledgments

This study was supported by funding from the National Institutes of Health (1R01AI083269) and Juvenile Diabetes Research Foundation (33-2008-412) to R.T. C.K. was supported by a National Institutes of Health Training Grant (T32 AI007273). The UNC Flow Cytometry Core Facility is supported in part by P30 CA016086 Cancer Center Core Support Grant to the UNC Lineberger Comprehensive Cancer Center, and North Carolina Biotech Center Institutional Support Grant 2005-IDG-1016.

Abbreviations

AIRE	autoimmune regulator
Ag	antigen
APC	antigen presenting cells
CFSE	carboxyfluorescein diacetate succinmidyl ester
CatS	cathespin S, (c/p)DC, (conventional/plasmacytoid) dendritic cell
DP	double-positive thymocyte
HA	*influenza* hemagglutinin peptide
HEL	hen egg lysozyme
OVA	ovalbumin
SIRPα	signal regulatory protein alpha
SP	single-positive thymocyte
(m/c)TEC	(medullary/cortical) thymic epithelial cell
TSA	tissue-specific Ag
TSSP	thymus specific serine protease
T1D	type 1 diabetes

References

1. Kyewski B, Klein L. A central role for central tolerance. Annu Rev Immunol. 2006; 24:571–606. [PubMed: 16551260]
2. Surh CD, Sprent J. T-cell apoptosis detected in situ during positive and negative selection in the thymus. Nature. 1994; 372:100–103. [PubMed: 7969401]
3. Kishimoto H, Sprent J. A defect in central tolerance in NOD mice. Nat Immunol. 2001; 2:1025–1031. [PubMed: 11668341]
4. Pugliese A, Zeller M, Fernandez A Jr, Zalcberg LJ, Bartlett RJ, Ricordi C, Pietropaolo M, Eisenbarth GS, Bennett ST, Patel DD. The insulin gene is transcribed in the human thymus and transcription levels correlated with allelic variation at the INS VNTR-IDDM2 susceptibility locus for type 1 diabetes. Nat Genet. 1997; 15:293–297. [PubMed: 9054945]
5. Vafiadis P, Bennett ST, Todd JA, Nadeau J, Grabs R, Goodyer CG, Wickramasinghe S, Colle E, Polychronakos C. Insulin expression in human thymus is modulated by INS VNTR alleles at the IDDM2 locus. Nat Genet. 1997; 15:289–292. [PubMed: 9054944]
6. Serre L, Fazilleau N, Guerder S. Central tolerance spares the private high-avidity CD4 T-cell repertoire specific for an islet antigen in NOD mice. Eur J Immunol. 2015
7. Anderson MS, Bluestone JA. The NOD mouse: a model of immune dysregulation. Annu Rev Immunol. 2005; 23:447–485. [PubMed: 15771578]
8. Derbinski J, Schulte A, Kyewski B, Klein L. Promiscuous gene expression in medullary thymic epithelial cells mirrors the peripheral self. Nat Immunol. 2001; 2:1032–1039. [PubMed: 11600886]
9. Anderson MS, Venanzi ES, Klein L, Chen Z, Berzins SP, Turley SJ, von Boehmer H, Bronson R, Dierich A, Benoist C, Mathis D. Projection of an immunological self shadow within the thymus by the aire protein. Science. 2002; 298:1395–1401. [PubMed: 12376594]
10. Liston A, Lesage S, Wilson J, Peltonen L, Goodnow CC. Aire regulates negative selection of organ-specific T cells. Nat Immunol. 2003; 4:350–354. [PubMed: 12612579]
11. Ohnmacht C, Pullner A, King SB, Drexler I, Meier S, Brocker T, Voehringer D. Constitutive ablation of dendritic cells breaks self-tolerance of CD4 T cells and results in spontaneous fatal autoimmunity. J Exp Med. 2009; 206:549–559. [PubMed: 19237601]
12. Kaneko T, Saito Y, Kotani T, Okazawa H, Iwamura H, Sato-Hashimoto M, Kanazawa Y, Takahashi S, Hiromura K, Kusakari S, Kaneko Y, Murata Y, Ohnishi H, Nojima Y, Takagishi K, Matozaki T. Dendritic cell-specific ablation of the protein tyrosine phosphatase Shp1 promotes Th1 cell differentiation and induces autoimmunity. J Immunol. 2012; 188:5397–5407. [PubMed: 22539788]
13. Wu L, Shortman K. Heterogeneity of thymic dendritic cells. Semin Immunol. 2005; 17:304–312. [PubMed: 15946853]
14. Koble C, Kyewski B. The thymic medulla: a unique microenvironment for intercellular self-antigen transfer. J Exp Med. 2009; 206:1505–1513. [PubMed: 19564355]
15. Hubert FX, Kinkel SA, Davey GM, Phipson B, Mueller SN, Liston A, Proietto AI, Cannon PZ, Forehan S, Smyth GK, Wu L, Goodnow CC, Carbone FR, Scott HS, Heath WR. Aire regulates the transfer of antigen from mTECs to dendritic cells for induction of thymic tolerance. Blood. 2011; 118:2462–2472. [PubMed: 21505196]
16. Atibalentja DF, Byersdorfer CA, Unanue ER. Thymus-blood protein interactions are highly effective in negative selection and regulatory T cell induction. J Immunol. 2009; 183:7909–7918. [PubMed: 19933868]
17. Atibalentja DF, Murphy KM, Unanue ER. Functional redundancy between thymic CD8alpha+ and Sirpalpha+ conventional dendritic cells in presentation of blood-derived lysozyme by MHC class II proteins. J Immunol. 2011; 186:1421–1431. [PubMed: 21178002]
18. Baba T, Nakamoto Y, Mukaida N. Crucial contribution of thymic Sirp alpha+ conventional dendritic cells to central tolerance against blood-borne antigens in a CCR2-dependent manner. J Immunol. 2009; 183:3053–3063. [PubMed: 19675159]
19. Li J, Park J, Foss D, Goldschneider I. Thymus-homing peripheral dendritic cells constitute two of the three major subsets of dendritic cells in the steady-state thymus. J Exp Med. 2009; 206:607–622. [PubMed: 19273629]

20. Proietto AI, van Dommelen S, Zhou P, Rizzitelli A, D'Amico A, Steptoe RJ, Naik SH, Lahoud MH, Liu Y, Zheng P, Shortman K, Wu L. Dendritic cells in the thymus contribute to T-regulatory cell induction. Proc Natl Acad Sci U S A. 2008; 105:19869–19874. [PubMed: 19073916]
21. Bonasio R, Scimone ML, Schaerli P, Grabie N, Lichtman AH, von Andrian UH. Clonal deletion of thymocytes by circulating dendritic cells homing to the thymus. Nat Immunol. 2006; 7:1092–1100. [PubMed: 16951687]
22. Hadeiba H, Lahl K, Edalati A, Oderup C, Habtezion A, Pachynski R, Nguyen L, Ghodsi A, Adler S, Butcher EC. Plasmacytoid dendritic cells transport peripheral antigens to the thymus to promote central tolerance. Immunity. 2012; 36:438–450. [PubMed: 22444632]
23. Klein L, Hinterberger M, von Rohrscheidt J, Aichinger M. Autonomous versus dendritic cell-dependent contributions of medullary thymic epithelial cells to central tolerance. Trends Immunol. 2011; 32:188–193. [PubMed: 21493141]
24. Gallegos AM, Bevan MJ. Central tolerance to tissue-specific antigens mediated by direct and indirect antigen presentation. J Exp Med. 2004; 200:1039–1049. [PubMed: 15492126]
25. He Q, Morillon YM 2nd, Spidale NA, Kroger CJ, Liu B, Sartor RB, Wang B, Tisch R. Thymic development of autoreactive T cells in NOD mice is regulated in an age-dependent manner. J Immunol. 2013; 191:5858–5866. [PubMed: 24198282]
26. Gagnerault MC, Lanvin O, Pasquier V, Garcia C, Damotte D, Lucas B, Lepault F. Autoimmunity during thymectomy-induced lymphopenia: role of thymus ablation and initial effector T cell activation timing in nonobese diabetic mice. J Immunol. 2009; 183:4913–4920. [PubMed: 19801516]
27. Huseby ES, Sather B, Huseby PG, Goverman J. Age-dependent T cell tolerance and autoimmunity to myelin basic protein. Immunity. 2001; 14:471–481. [PubMed: 11336692]
28. Markert ML, Devlin BH, McCarthy EA. Thymus transplantation. Clin Immunol. 2010; 135:236–246. [PubMed: 20236866]
29. Zucchelli S, Holler P, Yamagata T, Roy M, Benoist C, Mathis D. Defective central tolerance induction in NOD mice: genomics and genetics. Immunity. 2005; 22:385–396. [PubMed: 15780994]
30. Belizaire R, Unanue ER. Targeting proteins to distinct subcellular compartments reveals unique requirements for MHC class I and II presentation. Proc Natl Acad Sci U S A. 2009; 106:17463–17468. [PubMed: 19805168]
31. Schurich A, Bottcher JP, Burgdorf S, Penzler P, Hegenbarth S, Kern M, Dolf A, Endl E, Schultze J, Wiertz E, Stabenow D, Kurts C, Knolle P. Distinct kinetics and dynamics of cross-presentation in liver sinusoidal endothelial cells compared to dendritic cells. Hepatology. 2009; 50:909–919. [PubMed: 19610048]
32. Daro E, Pulendran B, Brasel K, Teepe M, Pettit D, Lynch DH, Vremec D, Robb L, Shortman K, McKenna HJ, Maliszewski CR, Maraskovsky E. Polyethylene glycol-modified GM-CSF expands CD11b(high)CD11c(high) but notCD11b(low)CD11c(high) murine dendritic cells in vivo: a comparative analysis with Flt3 ligand. J Immunol. 2000; 165:49–58. [PubMed: 10861034]
33. Janicka M, Chindemi PA, Hu WL, Regoeczi E. Effect of transferrin on the degradation of glycoproteins bearing a hybrid or high-mannose glycan by alveolar macrophages. Exp Cell Res. 1994; 215:17–22. [PubMed: 7957665]
34. Burgdorf S, Kautz A, Bohnert V, Knolle PA, Kurts C. Distinct pathways of antigen uptake and intracellular routing in CD4 and CD8 T cell activation. Science. 2007; 316:612–616. [PubMed: 17463291]
35. Dakic A, Shao QX, D'Amico A, O'Keeffe M, Chen WF, Shortman K, Wu L. Development of the dendritic cell system during mouse ontogeny. J Immunol. 2004; 172:1018–1027. [PubMed: 14707075]
36. Spidale NA, Wang B, Tisch R. Cutting edge: Antigen-specific thymocyte feedback regulates homeostatic thymic conventional dendritic cell maturation. J Immunol. 2014; 193:21–25. [PubMed: 24890722]
37. Viret C, Mahiddine K, Baker RL, Haskins K, Guerder S. The T Cell Repertoire-Diversifying Enzyme TSSP Contributes to Thymic Selection of Diabetogenic CD4 T Cell Specificities Reactive to ChgA and IAPP Autoantigens. J Immunol. 2015; 195:1964–1973. [PubMed: 26209627]

38. Viret C, Leung-Theung-Long S, Serre L, Lamare C, Vignali DA, Malissen B, Carrier A, Guerder S. Thymus-specific serine protease controls autoreactive CD4 T cell development and autoimmune diabetes in mice. J Clin Invest. 2011; 121:1810–1821. [PubMed: 21505262]

39. Driessen C, Bryant RA, Lennon-Dumenil AM, Villadangos JA, Bryant PW, Shi GP, Chapman HA, Ploegh HL. Cathepsin S controls the trafficking and maturation of MHC class II molecules in dendritic cells. J Cell Biol. 1999; 147:775–790. [PubMed: 10562280]

40. Nakagawa TY, Brissette WH, Lira PD, Griffiths RJ, Petrushova N, Stock J, McNeish JD, Eastman SE, Howard ED, Clarke SR, Rosloniec EF, Elliott EA, Rudensky AY. Impaired invariant chain degradation and antigen presentation and diminished collagen-induced arthritis in cathepsin S null mice. Immunity. 1999; 10:207–217. [PubMed: 10072073]

41. Shi GP, Villadangos JA, Dranoff G, Small C, Gu L, Haley KJ, Riese R, Ploegh HL, Chapman HA. Cathepsin S required for normal MHC class II peptide loading and germinal center development. Immunity. 1999; 10:197–206. [PubMed: 10072072]

42. Riese RJ, Mitchell RN, Villadangos JA, Shi GP, Palmer JT, Karp ER, De Sanctis GT, Ploegh HL, Chapman HA. Cathepsin S activity regulates antigen presentation and immunity. J Clin Invest. 1998; 101:2351–2363. [PubMed: 9616206]

43. Riese RJ, Wolf PR, Bromme D, Natkin LR, Villadangos JA, Ploegh HL, Chapman HA. Essential role for cathepsin S in MHC class II-associated invariant chain processing and peptide loading. Immunity. 1996; 4:357–366. [PubMed: 8612130]

44. Guerau-de-Arellano M, Martinic M, Benoist C, Mathis D. Neonatal tolerance revisited: a perinatal window for Aire control of autoimmunity. J Exp Med. 2009; 206:1245–1252. [PubMed: 19487417]

45. Klein L, Kyewski B. Self-antigen presentation by thymic stromal cells: a subtle division of labor. Curr Opin Immunol. 2000; 12:179–186. [PubMed: 10712940]

46. Dudziak D, Kamphorst AO, Heidkamp GF, Buchholz VR, Trumpfheller C, Yamazaki S, Cheong C, Liu K, Lee HW, Park CG, Steinman RM, Nussenzweig MC. Differential antigen processing by dendritic cell subsets in vivo. Science. 2007; 315:107–111. [PubMed: 17204652]

47. Dresch C, Ackermann M, Vogt B, de Andrade Pereira B, Shortman K, Fraefel C. Thymic but not splenic CD8(+) DCs can efficiently cross-prime T cells in the absence of licensing factors. Eur J Immunol. 2011; 41:2544–2555. [PubMed: 21748731]

48. Sands MS, Barker JE. Percutaneous intravenous injection in neonatal mice. Lab Anim Sci. 1999; 49:328–330. [PubMed: 10403452]

49. Johnson MC, Garland AL, Nicolson SC, Li C, Samulski RJ, Wang B, Tisch R. beta-cell-specific IL-2 therapy increases islet Foxp3+Treg and suppresses type 1 diabetes in NOD mice. Diabetes. 2013; 62:3775–3784. [PubMed: 23884888]

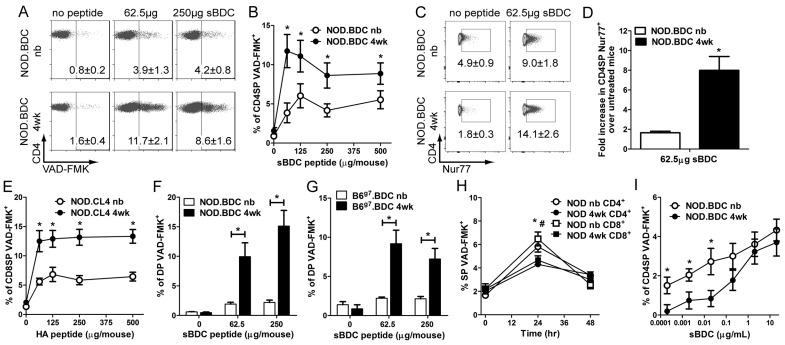

Figure 1. The efficiency of peptide-induced negative selection increases with age

Newborn and 4 wk-old (A–D) NOD.BDC, mice were injected i.v. with sBDC peptide and the frequency of (A,B) VAD-FMK$^+$ and (C,D) Nur77$^+$ CD4SP thymocytes determined via flow cytometry. (D) The fold increase in Nur77$^+$ CD4SP of sBDC-treated versus untreated 4 wk-old and newborn animals. (A,B) Data ± SEM are the average of ≥3 separate experiments, with ≥4 mice/peptide dose; *p<0.05 (paired Student's t-test). (C,D) Data ± SEM are the average of 2 separate experiments, n≥6 mice/group; *p<0.05 (paired Student's t-test). (E) NOD.CL4 newborn and 4 wk-old mice were injected i.v. with HA peptide and the frequency of VAD-FMK$^+$ CD8SP thymocytes determined via flow cytometry. Data ± SEM are the average of ≥3 separate experiments with 3 untreated mice and ≥ 5 mice/peptide dose; *p<0.05 (paired Student's t-test). (F) NOD.BDC and (G) B6^{g7}.BDC newborn and 4 wk-old mice were injected with sBDC peptide i.v., and the percent of VAD-FMK$^+$ DP detected by flow cytometry. Data ± SEM are the average of ≥3 separate experiments, with ≥4 NOD and 6 B6^{g7}.BDC mice per group tested; *p<0.05 (paired Student's t-test). (H) Frequency of VAD-FMK$^+$ SP in NOD newborn or 4 wk-old mice injected with 12.5 mg/kg of dexamethasone measured by flow cytometry; the data ± SEM are the average of 2 separate experiments analyzing ≥5 animals (*,# p<0.05 Student's t-test for CD4 and CD8SP, respectively). (I) *In vitro* peptide-induced apoptosis in NOD.BDC newborn and 4 wk-old thymocytes was determined via flow cytometry. Data ± SEM are the average of ≥3 separate experiments examining ≥9 mice; *p<0.05 (paired Student's t-test).

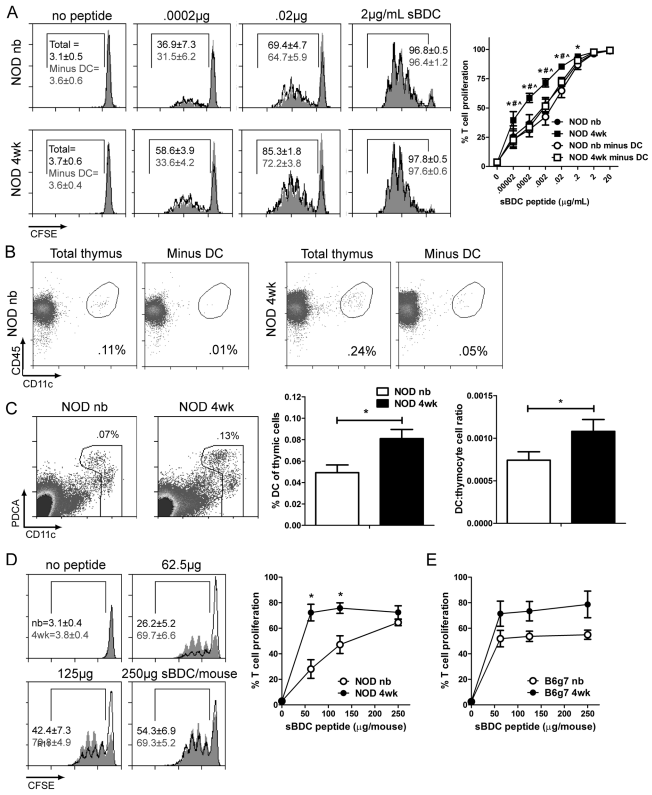

Figure 2. Thymic DC stimulatory capacity increases in a temporal manner

(A) CFSE-labeled NOD.BDC CD4$^+$ T cells were co-cultured with sBDC pulsed NOD newborn or 4 wk-old thymus cell suspensions ± CD11c$^+$ cells at a 1:10 cell ratio (n=6–8 mice). $^*p<0.05$ (paired Student's t test), total newborn versus 4 wk-old peptide pulsed thymic suspensions; $^{\#}/^{\wedge}p<0.05$ (paired Student's t test) total 4 wk-old versus DC-depleted 4 wk-old and newborn peptide pulsed thymic suspensions, respectively. (B) DC frequency in NOD newborn and 4 wk-old thymus suspensions prior to and after anti-CD11c bead depletion; data are representative of 3 separate experiments. (C) DC frequency and the ratio of DC to thymocytes in newborn and 4 wk-old thymi (n≥10 mice/group). (D) T cell proliferation induced by thymic DC isolated from NOD mice injected with sBDC or left untreated, and co-cultured with CFSE-labeled NOD.BDC CD4$^+$ T cells. Data ± SEM are the average of 4 separate experiments. *p<0.05 (paired Student's t-test). (E) T cell stimulatory capacity of newborn and 4 wk-old bulk thymic DC isolated from B6^{g7} mice injected with different doses of sBDC peptide, and cultured with CFSE-labeled NOD.BDC CD4$^+$ T cells (n=2–3 mice/group).

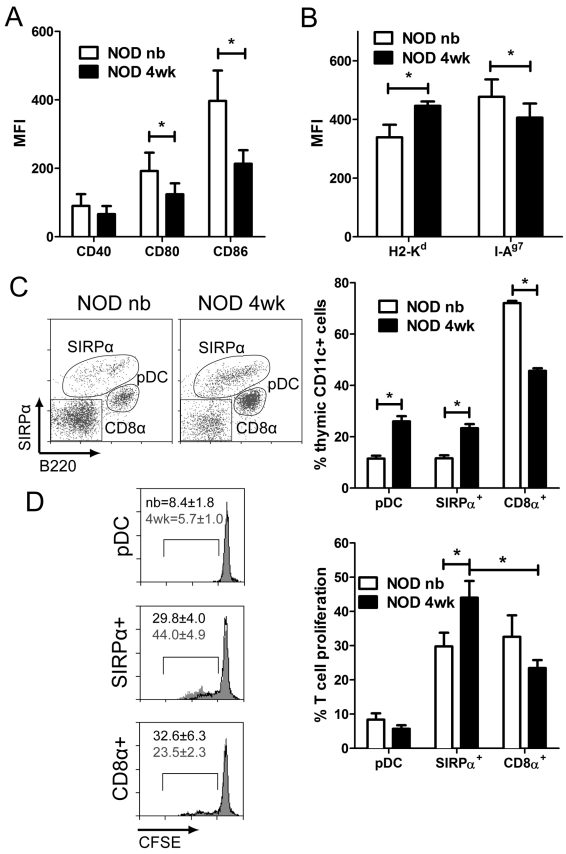

Figure 3. SIRPα$^+$ DC are increased in the 4 wk-old thymus and exhibit enhanced T cell stimulatory capacity

Expression of (A) co-stimulatory and (B) MHC molecules by NOD newborn and 4 wk-old thymic DC; data ± SEM are the average of ≥4 separate experiments. (C) Frequency of NOD newborn and 4 wk-old thymic DC subsets (n=7 mice). (D) T cell stimulation by newborn versus 4 wk-old thymic DC subsets sorted from NOD mice, injected with 10 μg sBDC, and cultured with CFSE-labeled NOD.BDC CD4$^+$ T cells; data ± SEM are the average of 12 separate samples. *p<0.05 (paired Student's t-test).

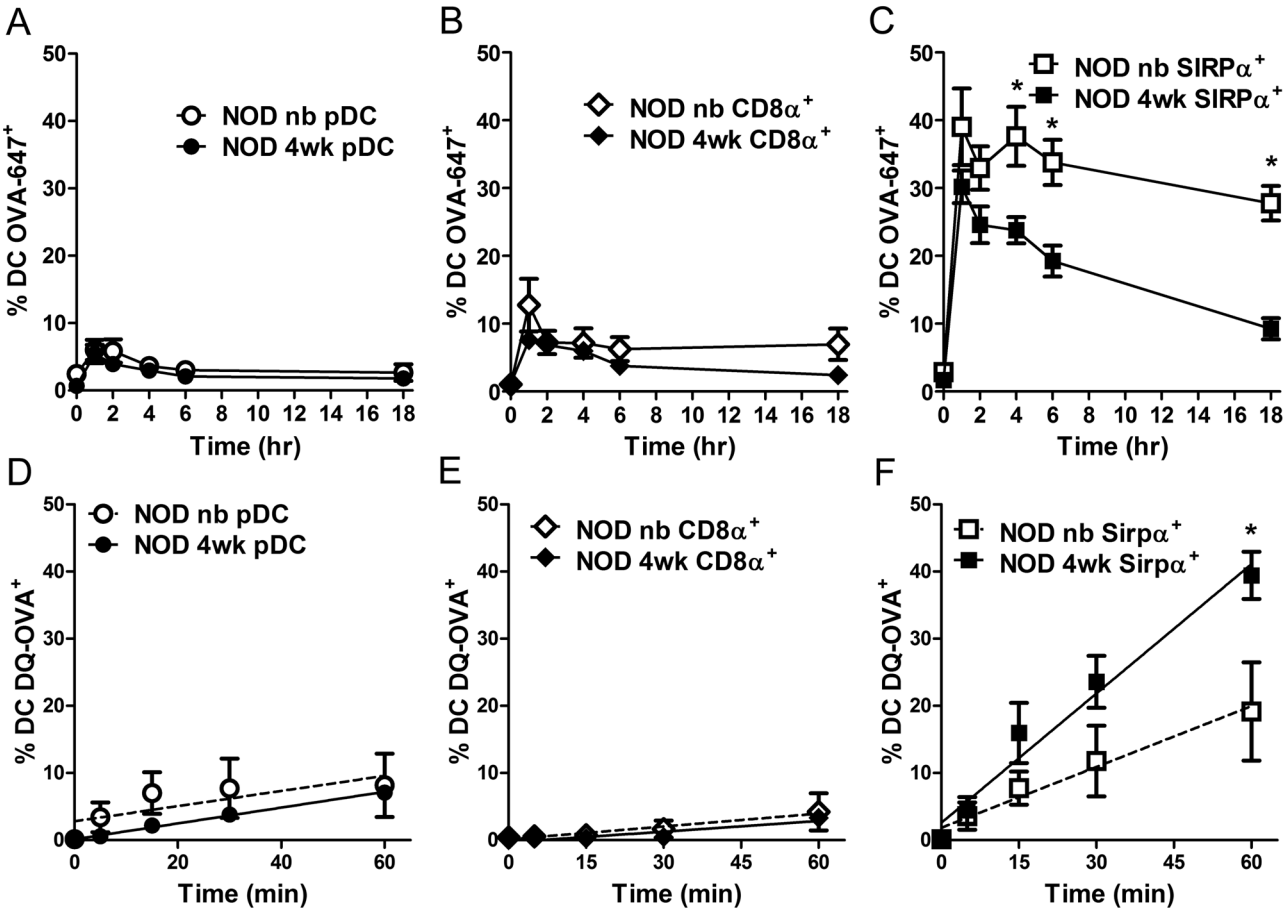

Figure 4. 4 wk-old thymic SIRPα$^+$ DC exhibit enhanced antigen processing and presentation properties

Percent of OVA-647$^+$ thymic (A) pDC, (B) CD8α$^+$, and (C) SIRPα$^+$ from newborn or 4 wk-old NOD mice injected with 2.7 mg/kg (3.5 μg or 50 μg respectively) of OVA-647 (n≥ 8 mice/group) at different times post injection. (D–F) Frequency of fluorescent thymic DC from newborn and 4 wk-old NOD mice treated with 0.5 μg/well DQ-OVA *in vitro*. Data ± SEM are the average of 4 separate experiments. *p<0.05 (A–C, Student's t-test; D–F, linear regression analysis).

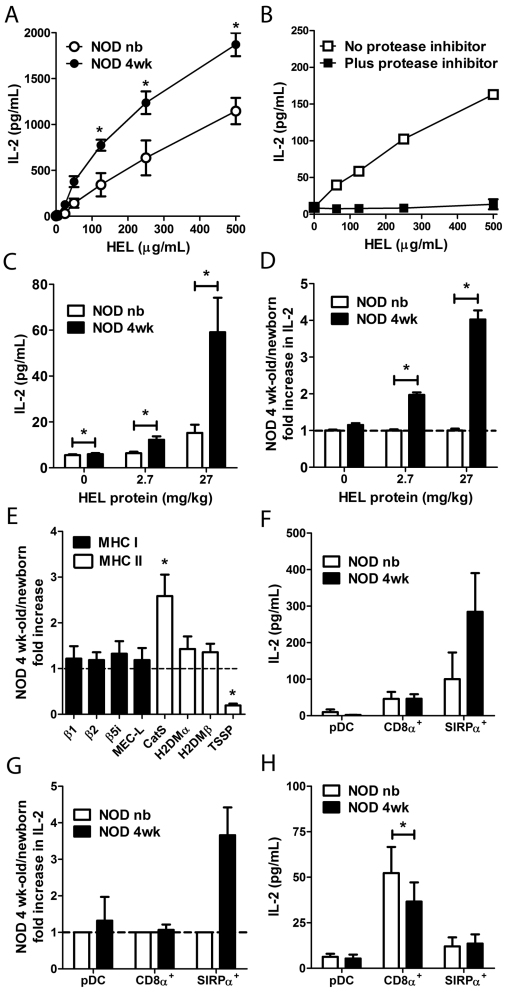

Figure 5. 4 wk-old SIRPα$^+$ DC demonstrate enhanced Ag processing and T cell stimulation

Newborn and 4 wk-old NOD thymic DC (A–E) in bulk or (F–H) flow-sorted subsets were tested for inducing IL-2 secretion by (A–D, F, G) Clone 4 CD4$^+$ or (H) 8c11 CD8$^+$ HEL-specific T cells. (A,B, F–H) Thymic DC were pulsed with (A,B) varying concentrations, (F,G) 125 μg/ml, or (H) 500 μg/ml of HEL protein *in vitro*, or (C,D) isolated from newborn and 4 wk-old NOD mice injected i.v. with 2.7 or 27 mg/kg body weight of HEL, respectively. (B) IL-2 induced secretion following pre-treatment of NOD 4 wk-old thymic DC with a protease inhibitor cocktail. (D,G) Fold increase in IL-2 production induced by 4 wk-old versus newborn thymic DC with the newborn values equal to 1. (E) Relative expression of MHC I and II protein processing molecules in NOD newborn and 4 wk-old thymic DC determined by real-time PCR. (H) Sorted thymic DC subsets were co-cultured with 500 μg/mL HEL protein plus Clone 8c11 CD8$^+$ T cells and IL-2 measured. Data ± SEM of n=2 (B,F,G), n=3 (A,C,D,H), n=4–5 (E) separate experiments are depicted. *p<0.05 (Student's paired t-test).